# Ubiquitin-proteasomes are the dominant mediators of the regulatory effect of microRNA-1 on cardiac remodeling after myocardial infarction

LIPING WEI[1*], YUFAN ZHANG[2*], XIN QI[1], XUSENG SUN[2], YUANYANG LI[3] and YUE XU[3]

[1]Department of Cardiology, Tianjin Union Medical Center, Nankai University Affiliated Hospital, Tianjin 300121; [2]School of Graduate Studies, Tianjin Medical University, Tianjin 300070; [3]School of Graduate Studies, Tianjin University of Traditional Chinese Medicine, Tianjin 300193, P.R. China

Received January 16, 2019; Accepted August 20, 2019

DOI: 10.3892/ijmm.2019.4330

**Abstract.** Patients with ischemic hearts who have refused coronary vascular reconstruction may exhibit dynamic myocardial remodeling and cardiac dysfunction. In the present study, the role of miRNA-1 and its association with the ubiquitin-proteasome system (UPS) in regulating myocardial remodeling was investigated. A myocardial infarction (MI) model was constructed and the hearts were treated with miRNA-1 antagomir, miRNA-1 lentiviral vectors and the UPS proteasome blocker bortezomib. The expression levels of miRNA-1 were evaluated using reverse transcription PCR and the abundance of the ubiquitin-proteasome protein and caspase-3 were evaluated via western blot analysis. Furthermore, the collagen volume fraction was calculated using Masson's trichrome staining, and the apoptosis index was detected via terminal deoxynucleotidyl transferase dUTP-biotin nick end labeling staining. Transforming growth factor (TGF)-β expression was assessed via immunohistochemical staining. Echocardiographic characteristics and myocardial infarct size were analyzed. miRNA-1 expression levels were found to be increased following MI. miRNA-1 antagomir administration clearly inhibited miRNA-1 expression, whereas the miRNA-1 lentiviral vector exerted the opposite effect. The levels of 19s proteasome, 20S proteasome and ubiquitin ligase E3 were decreased in the miRNA-1 antagomir group, but were significantly increased in the miRNA-1 lentiviral group; however, only 20S proteasome expression was decreased in the bortezomib group. Collagen hyperplasia and TGF-β expression were decreased in both the miRNA-1 antagomir and bortezomib groups, although the effects of the miRNA-1 antagomir were more noticeable. The miRNA-1 antagomir and the UPS proteasome blocker both alleviated the ultrastructural impairments, demonstrated by a decreased left ventricular (LV) end-diastolic diameter and LV mass, but the miRNA-1 antagomir was also able to increase LV ejection fraction and LV fractional shortening. miRNA-1 regulated UPS-associated mRNA expression and affected the majority of the UPS components in the myocardium, thereby leading to increased myocardial cell apoptosis, myocardial fibrosis and remodeling. The miRNA-1 antagomir exerted a more prominent cardioprotective effect compared with the UPS proteasome blocker bortezomib.

*Correspondence to:* Dr Liping Wei, Department of Cardiology, Tianjin Union Medical Center, Nankai University Affiliated Hospital, 190 Jieyuan Road, Hongqiao, Tianjin 300121, P.R. China
E-mail: weilipingme@163.com; weilipingme123@163.com

*Contributed equally

*Key words:* miRNA-1, myocardial remolding, ubiquitin proteasome system, apoptosis

## Introduction

Patients with ischemic hearts exhibit progressive myocardial remodeling, which is associated with massive cardiomyocyte loss, and for which an ideal therapeutic approach has yet to be identified (1,2). The pathological changes associated with ischemic hearts primarily involve cardiomyocyte apoptosis and myocardial fibrosis. The myocardial remodeling process includes myocardial cell apoptosis, necrosis, subsequent tissue fibrosis and, ultimately, heart failure, which is an inevitable consequence when patients are not treated in a timely manner, or if the patients cannot be revascularized (3). Substitution of apoptotic cardiomyocytes by collagen and fibrous tissue is an important cause of heart failure progression and myocardial remodeling. Stem cells and gene therapy may represent new strategies for blocking cardiac remodeling before it commences (4). It is advisable to prevent the progression of heart failure that occurs as a result of myocardial lesions by altering microRNA (miRNA) expression levels.

miRNAs are endogenous, non-coding small RNAs that regulate target genes at the post-transcriptional level and have been found to play an upstream regulatory role in the pathogenesis of heart failure (5-7). The most abundant miRNA in cardiac myocytes, and also the first miRNA to be implicated in heart development, is miRNA-1 (8,9). Accumulating

evidence has demonstrated that cardiomyocyte apoptosis is closely associated with the abnormal expression of miRNA-1. Activation of caspases plays a central role in the execution phase of cell apoptosis (10), and caspase-3 is considered as the executioner of apoptosis. Previous studies demonstrated that there is a crucial interrelationship between caspase-3 activation and functional reserve in cardiomyocytes (11). It was also previously reported that miRNAs target caspase-3 in PANC-1 cells (12).

The expression of the UPS components, such as E2 conjugating enzymes, E3 ubiquitin ligases, or subunits of the proteasome, are either increased or decreased in cardiac disease. The expression levels of the UPS components are high in the impaired myocardium, and may be responsible for the degradation of the majority of senescent cellular proteins, as well as playing a key role in DNA repair (13-15). As defective protein degradation in human cardiomyopathies has been established, recent studies have started to address the potential underlying mechanisms. The overall observed increase in the expression of ubiquitination machinery in failing hearts may be in response to an increased protein burden, which may be attributed to the increased protein synthesis that accompanies the hypertrophic response, or to an excess of damaged or modified proteins to be targeted for proteasomal degradation (16,17). The association between these two systems remains to be fully elucidated.

The aim of the present study was to investigate the expression levels of miRNA-1 in mice with acute heart failure induced by acute ischemia, elucidate the role of miRNA-1 in myocardial remodeling and determine whether there is an association with the ubiquitin-proteasome system (UPS) in the regulation of heart remodeling following myocardial infarction (MI).

## Materials and methods

*MI model construction*. A total of 48 male C57BL/6 mice, aged 6 weeks and weighing 25-30 g, were used in the present study. All animals were housed in an air-conditioned room (22±0.5˚C) under a 12/12 h light-dark cycle with access to standard laboratory food and water *ad libitum*. After the mice were anesthetized by inhaling 2% isoflurane, a skin incision was made over the left chest, followed by tying a slipknot around one-third of the left anterior descending artery. The sham group underwent the same surgical procedure, except the suture placed under the left coronary artery was not tied. A control vector (30 $\mu$l), an miRNA-1 antagomir (30 $\mu$l, 1x$10^9$ TU/ml), an miRNA-1 lentiviral vector (30 $\mu$l, 1x$10^9$ TU/ml) and bortezomib (30 $\mu$l, 0.5 mg/kg) were delivered via intramyocardial injections, temporarily blanching the left ventricular (LV) anterior wall. The 48 mice were divided into the following groups (n=8 per group): i) Sham; ii) MI; iii) MI + control vector; iv) MI + miRNA-1 antagomir; v) MI + miRNA-1 lentiviral vector; and vi) MI + bortezomib. The protocol of the present study was approved by the Animal Ethics Committee of Tianjin Union Medical Center.

*Antagomir of miRNA-1 and overexpression of miRNA-1*. The antagomir method was used to block the expression of miRNA-1. A sequence of antisense oligonucleotides was designed (antagomir); the antisense nucleic acid was allowed to interact with the target miRNA, and then this was specifically intervened for downstream regulation. The miRNA-1 gene was overexpressed using lentiviral vectors. The small RNA gene and its side sequence were amplified from the genome and then cloned into lentiviral vectors. The lentivirus was named pPS-EF1-copGFP-LCS, and the reporter gene was green fluorescent protein (GFP); the antagomir and lentivirus were injected into the MI area and surrounding tissues. The antagomir and lentivirus were synthesized by Shanghai Ji Ma Biotechnology Co., Ltd.

*Western blot assay evaluation*. Total protein was extracted from tissues to detect the levels of caspase-3, 19S proteasome, 20S proteasome and ubiquitin ligase E3 in target tissue via western blotting. The proteins were separated via 12% SDS-PAGE, blotted and probed with rabbit anti-caspase-3 (1:500; Sigma-Aldrich; Merck KGaA; cat. no. C8487), rabbit anti-19S proteasome (1:1,000; Enzo Life Sciences; cat. no. Q9SEI2), rabbit anti-20S proteasome (1:1,000; Abcam; cat. no. ab22673) and rabbit anti-enzyme E3 (1:1,000; Abcam; cat. no. ab84067). A Bradford assay (Bio-Rad Laboratories, Inc.) was used to quantify protein concentrations. The blots were visualized using a chemiluminescence system (Amersham Bioscience; GE Healthcare).

*Determination of myocardial cell apoptosis*. Myocardial cell apoptosis was determined via terminal deoxyribonucleotidyl transferase-mediated dUTP-biotin nick end labeling (TUNEL) staining, as previously described (18,19).

*Masson's trichrome staining*. Masson's trichrome staining was performed for histopathological observation. Following inhalation of 2% isoflurane, the hearts of the mice were isolated, perfused with normal saline followed by 4% paraformaldehyde for fixation, dehydrated with ethanol, coronally sectioned into halves along the long axis, embedded in paraffin blocks, consecutively cut into 5-$\mu$m sections, and then treated with commercial reagents for Masson's trichrome staining. Muscle fibers were stained purple-red, while collagen fibers were stained green-blue. Collagen volume fraction, calculated from Masson's trichrome staining images, was expressed as a percentage of the total LV myocardial volume.

*Immunohistochemical staining*. The expression of transforming growth factor (TGF)-β in the process of MI was observed via immunohistochemistry, which further revealed the degree of myocardial fibrosis and myocardial remodeling. Paraffin-embedded heart sections were used for the staining. Briefly, the sections were dewaxed, microwaved to retrieve antigens, blocked with 5% BSA, incubated overnight at 4˚C with an isotype IgG control antibody, or with a rabbit anti-TGF-β (1:1,000; Cell Signaling Technology, Inc.; cat. no. 3711), and then hybridized with horseradish peroxidase-labeled secondary antibodies, followed by a 3,30-diaminobenzidine (DAB) chromogenic reaction. The brown DAB deposits were observed under a microscope.

*Measurement of infarct size*. After 2 weeks, the heart was frozen at -80˚C and sliced transversely into 1-mmsections. The

infarct size area (white area) and LV area were measured digitally using the Image Pro Plus software (Media Cybernetics, Inc.). Infarct size was expressed as a percentage of the white area/LV area.

*Echocardiographic examination*. After 2 weeks, echocardiography was performed using a high-resolution ultrasound imaging system. Anesthesia was induced with isoflurane 2% in 100% oxygen in an induction chamber. The sedated mice were studied using an echocardiography system (Sequoia Acuson, 15-MHz linear transducer; Siemens AG). The cardiac dimensions and function were assessed using M-mode echocardiography. LV end-diastolic diameter (LVDD) and LV end-systolic diameter were measured on the parasternal LV long axis view. LV fractional shortening (LVFS) was measured via the short axis view of the LV. LV ejection fraction (LVEF) and LV mass were calculated using computer algorithms. All measurements represent the mean of 5 consecutive cardiac cycles. All measurements were performed in a blinded manner.

*Statistical analysis*. All values and are expressed as mean ± standard deviation. Comparison between groups was subjected to analysis of variance followed by Tukey's multiple comparison test. Two-sided tests were used and $P<0.05$ was considered to indicate a statistically significant difference. SPSS software (version 23.0; IBM Corp.) was used for the data analysis.

## Results

*Expression levels of miRNA-1 following miRNA-1 antagomir, miRNA-1 lentiviral vectors and bortezomib treatment*. miRNA-1 antagomir, miRNA-1 lentiviral vector and the UPS proteasome blocker bortezomib were delivered via three separate intramyocardial injections. After 2 weeks, the border area tissue of the myocardial infarct from different groups was obtained in order to detect the miRNA-1 expression levels. miRNA-1 antagomir and miRNA-1 lentiviral models were successfully constructed and assessed via reverse transcription PCR. miRNA-1 expression levels were found to be significantly increased in the MI group ($P<0.01$) compared with the sham group (Fig. 1B). miRNA-1 expression was significantly decreased in the miRNA-1 antagomir group ($P<0.01$), whereas it was increased in the miRNA-1 lentiviral group ($P<0.01$). There was no significant difference between the bortezomib and control groups (Fig. 1B).

*Expression levels of the UPS components following alterations in miRNA-1 expression and administration of bortezomib*. The expression levels of the main component of the ubiquitin-proteasome, the 19S proteasome, were significantly increased in the MI group ($P<0.01$) compared with the sham group (Fig. 1A and C). The expression levels of the 19S proteasome were significantly decreased in the miRNA-1 antagomir group ($P<0.05$), increased in the miRNA-1 lentiviral group ($P<0.05$), and not significantly different in the bortezomib group when compared with the control group (Fig. 1A and C).

The expression levels of the 20S proteasome in the MI group were significantly increased ($P<0.01$) compared with those in the sham group (Fig. 1A and D). In addition, the 20S proteasome expression levels were significantly decreased in the miRNA-1 antagomir group ($P<0.01$), increased in the miRNA-1 lentiviral group ($P<0.05$), and also decreased in the bortezomib group ($P<0.01$) when compared with the control group (Fig. 1A and D).

The ubiquitin ligase E3 expression levels in the MI group were significantly increased ($P<0.01$) compared with those in the sham group (Fig. 1A and E). E3 expression was significantly decreased in the miRNA-1 antagomir group ($P<0.01$), significantly increased in the miRNA-1 lentiviral group ($P<0.01$), and not significantly different in the bortezomib group compared with the control group (Fig. 1A and E).

*TUNEL staining following interference with the miRNA-1 expression levels and inhibition of the UPS*. The number of apoptotic cells observed via TUNEL staining was significantly elevated in the MI group ($P<0.01$) compared with that in the sham group (Fig. 2A and B). The extent of apoptosis was significantly decreased in the miRNA-1 antagomir group ($P<0.05$), and there was no significant difference in the bortezomib group compared with in the control group. The extent of apoptosis in the miRNA-1 lentiviral group was significantly increased ($P<0.05$) compared with the control group (Fig. 2A and B).

*Caspase-3 expression following interference with the miRNA-1 expression levels and inhibition of the UPS*. The expression levels of caspase-3 during MI were evaluated using western blotting, which further demonstrated the degree of myocardial cell in the different groups. Caspase-3 expression levels in the MI area were markedly increased in the MI group ($P<0.01$) compared with the sham group (Fig. 2C). Caspase-3 expression levels in the miRNA-1 antagomir group were markedly decreased ($P<0.05$), and there was no significant difference in the bortezomib group compared with the control group. The caspase-3 expression levels in the miRNA-1 lentiviral group were significantly higher ($P<0.05$) compared with those in the control group (Fig. 2C).

*Masson's staining following interference with miRNA-1 expression and administration of bortezomib*. Masson's trichrome staining was used to assess the degree of myocardial fibrosis. Microscopic examination revealed that the myocardial tissue was purple-red in color, whereas the fibrous tissue was green-blue. The myocardial fibers in the sham operation group were arranged in a regular manner; there were no abnormalities in the myocardial interstitium or myocardial intravascular region. Collagen hyperplasia, myocardial fiber disorder, and the proportion of green-blue-stained collagen was markedly increased in the MI group ($P<0.01$) compared with those areas in the sham group (Fig. 3A and B). Collagen hyperplasia and myocardial fiber disarray were markedly decreased in the miRNA-1 antagomir ($P<0.01$) and bortezomib ($P<0.05$) groups, but the bortezomib group exhibited fewer changes. Furthermore, collagen hyperplasia and myocardial fiber disarray were observed in the miRNA-1 lentiviral group. The fractional collagen volume in the miRNA-1 lentiviral group was significantly higher ($P<0.01$) compared with that in the control group (Fig. 3A and B).

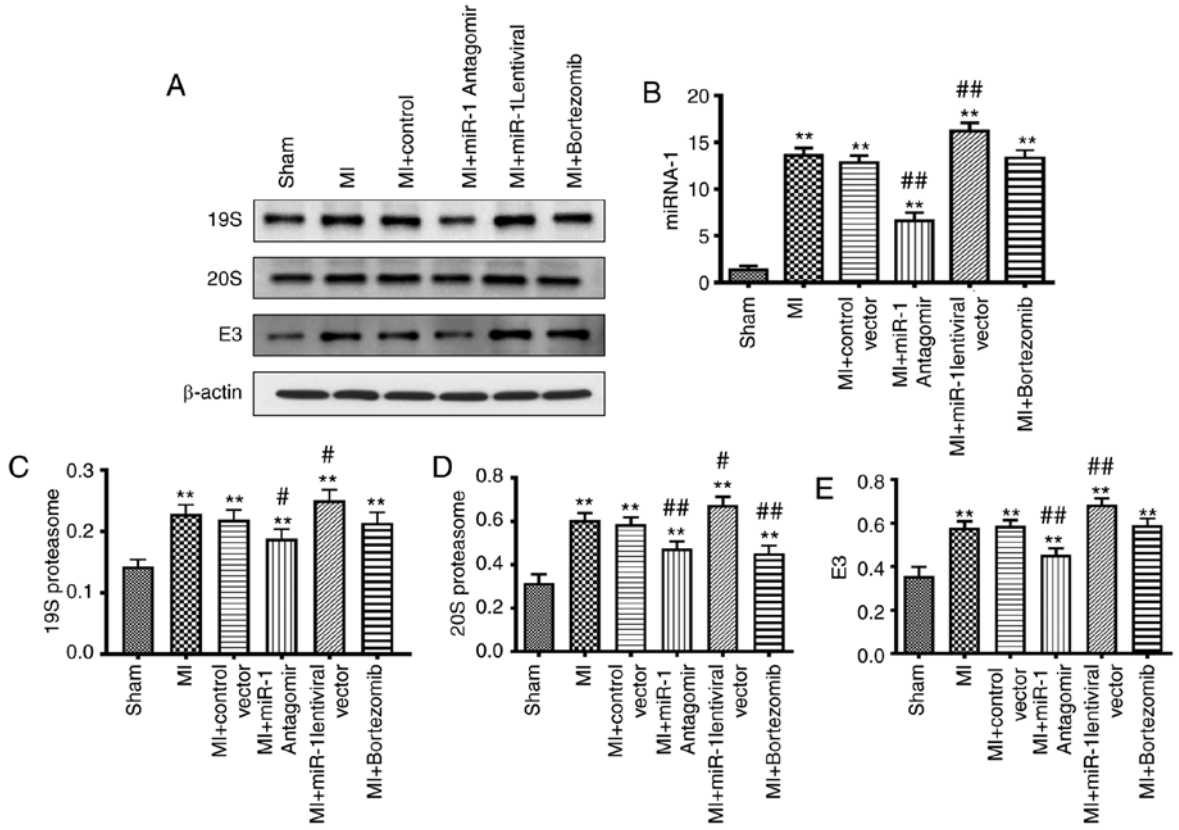


Figure 1. Expression of miRNA-1 and ubiquitin-proteasome protein. Ubiquitin-proteasome protein expression with representative gel blots and β-actin (loading control). (A) miRNA-1 expression levels as evaluated via reverse transcription PCR analysis. (B) 19S proteasome. (C) 20S proteasome. (D) Ubiquitin ligase E3. (E) Expression levels as evaluated via western blot analysis. Columns and bars represent mean and standard deviation. n=8 mice per group. $^{**}$P<0.01 vs. sham group; $^{\#}$P<0.05, $^{\#\#}$P<0.01 vs. MI + control vector group. MI, myocardial infarction.

*TGF-β expression levels following interference with miRNA-1 expression levels and inhibition of the UPS*. The expression levels of TGF-β during the MI were observed via immunohistochemistry, which further demonstrated the degree of myocardial fibrosis and myocardial remodeling. The TGF-β expression levels in the MI area were significantly increased in the MI group (P<0.01) compared with those in the sham group (Fig. 4A and B). The TGF-β expression levels in the miRNA-1 antagomir group were significantly decreased (P<0.01) compared with those in the control group, and were also significantly decreased in the bortezomib group (P<0.01). However, the TGF-β expression levels in the miRNA-1 lentiviral vector were significantly higher (P<0.01) compared with those in the control group (Fig. 4A and B).

*miRNA-1 antagomir decreases infarct size in mice following MI*. Infarct size was markedly higher in the MI group (P<0.01) compared with the sham group (Fig. 5A and B). Infarct size was markedly decreased in the miRNA-1 antagomir group (P<0.01), but was significantly larger in the miRNA-1 lentiviral group (P<0.01). There was no significant difference in the infarct size between the bortezomib and control groups (Fig. 5A and B).

*Cardiac function changes following interference with miRNA-1 expression levels and inhibition of the UPS*. The echocardiographic parameters revealed that LVEF (Fig. 2A and B), LVFS (Fig. 6A and C), LV mass (Fig. 6A and D) and LVDD (Fig. 6A and E) in the MI group exhibited significant changes (P<0.01) compared with the sham group. LVEF (Fig. 6A and B) and LVFS (Fig. 6A and C) were significantly increased in the miRNA-1 antagomir group (P<0.01), whereas LVEF (Fig. 6A and B) and LVFS (Fig. 6A and C) were decreased in the miRNA-1 lentiviral group (P<0.05), and were not significantly different in the bortezomib group compared with the control group.

LV mass (Fig. 6A and D) and LVDD (Fig. 6A and E) were significantly decreased in the miRNA-1 antagomir group (P<0.05), increased in the miRNA-1 lentiviral group (P<0.05), and mildly decreased in the bortezomib group (P<0.05) compared with the control group.

## Discussion

Previous studies (20-22) support the hypothesis that miRNAs may play an important role in the upstream regulation of heart failure progression; however, the role of miRNAs in physiological and pathophysiological processes in the heart remains elusive.

The most abundant miRNA in cardiac myocytes, and the first miRNA to be implicated in heart development, is miRNA-1. miRNA-1 is encoded by two almost identical genes: miRNA-1-1 and miRNA-1-2, which are located within introns 2 and 12 of the E3 ubiquitin-protein ligase (23). Mice lacking the miR-1-2 gene develop various heart abnormalities.

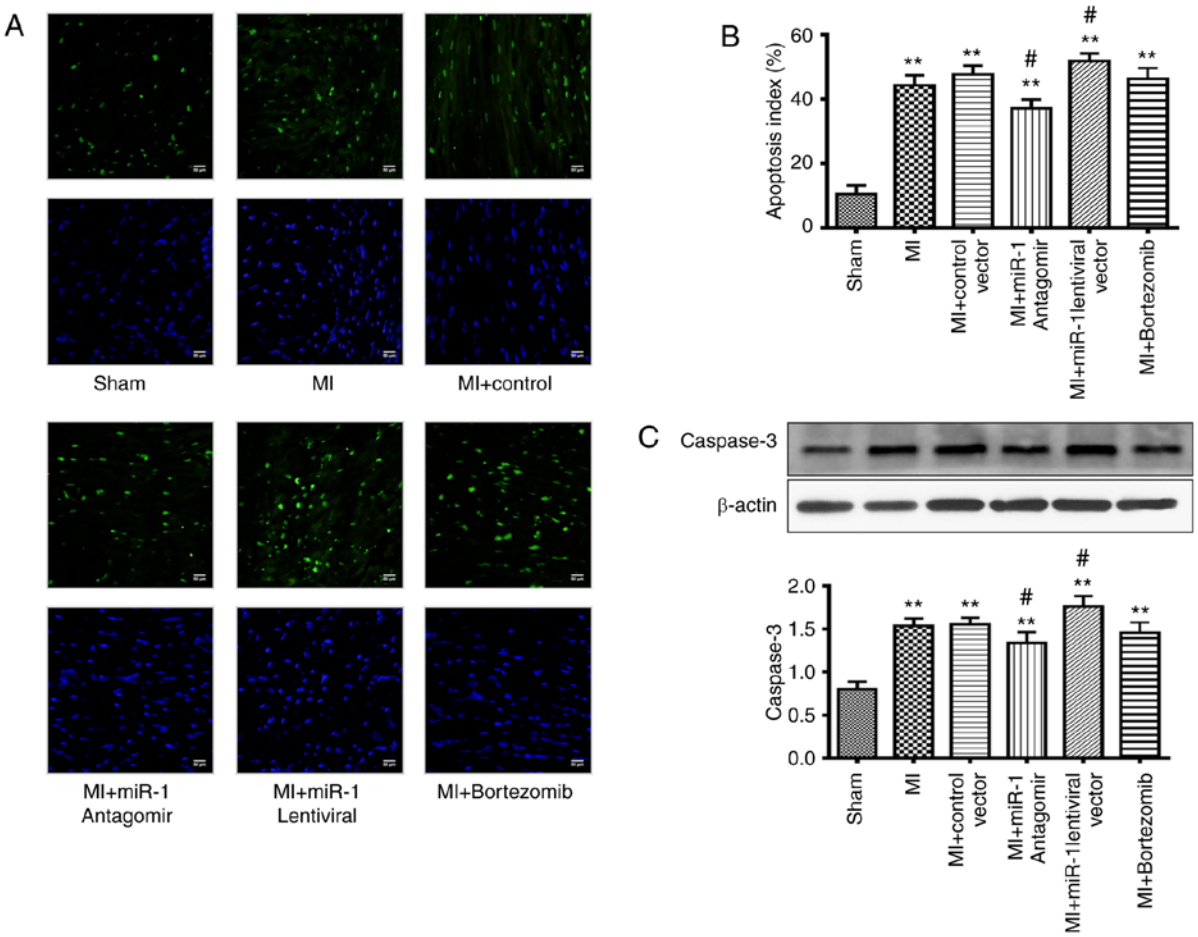


Figure 2. Extent of cell apoptosis in each group. (A) TUNEL-positive cardiomyocytes appear as green. (B) Quantitative analysis of apoptotic cardiomyocytes isolated from myocardial cardiac tissue in different groups. The index of apoptosis was equal to the number of TUNEL-positive cells divided by the total cells per field. (C) Protein expression with representative gel blots of caspase-3 and β-actin. The columns and error bars represent means and standard deviation. n=8 mice per group. $^{**}$P<0.01 vs. sham group; $^{\#}$P<0.05 vs. MI + control vector group. TUNEL, terminal deoxyribonucleotidyl transferase-mediated dUTP-biotin nick end labelling; MI, myocardial infarction.

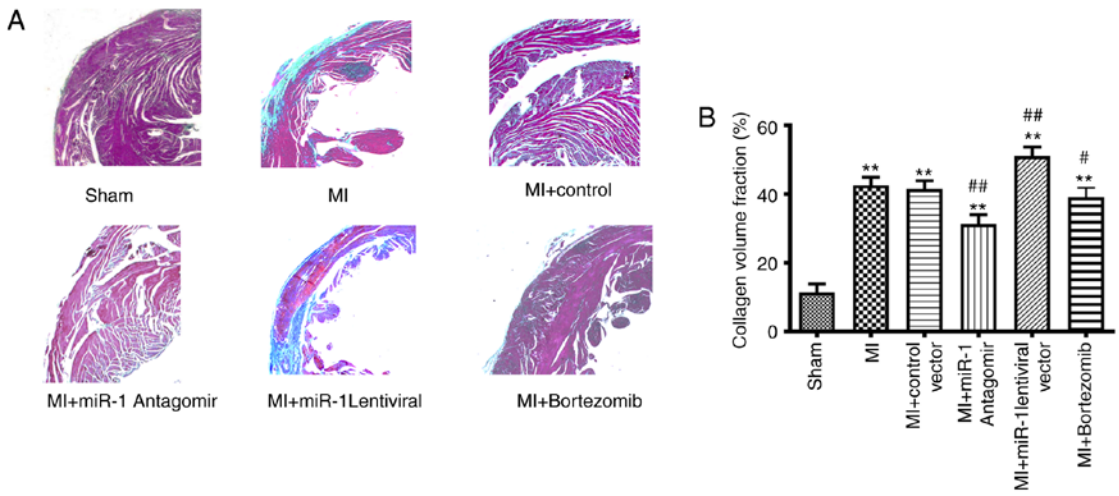


Figure 3. Analysis of Masson's trichrome staining. Representative microscopic images of heart sections following Masson's trichrome staining. (A) Collagen volume fraction calculated from Masson's trichrome staining images, expressed as a percentage of the total left ventricular myocardial volume. (B) n=8 mice per group. $^{**}$P<0.01 vs. sham group; $^{\#}$P<0.05; $^{\#\#}$P<0.01 vs. MI + control vector group. MI, myocardial infarction.

Accumulating evidence suggests that cardiomyocyte apoptosis is associated with abnormal expression of miRNA-1. miRNAs that are present in the early phases of myocardial ischemia may be associated with cell death and oxidative stress (24). Transplanting miRNA-1-transfected embryonic stem cells (miRNA-1-1-ES) into the border zone of the infarct in mice

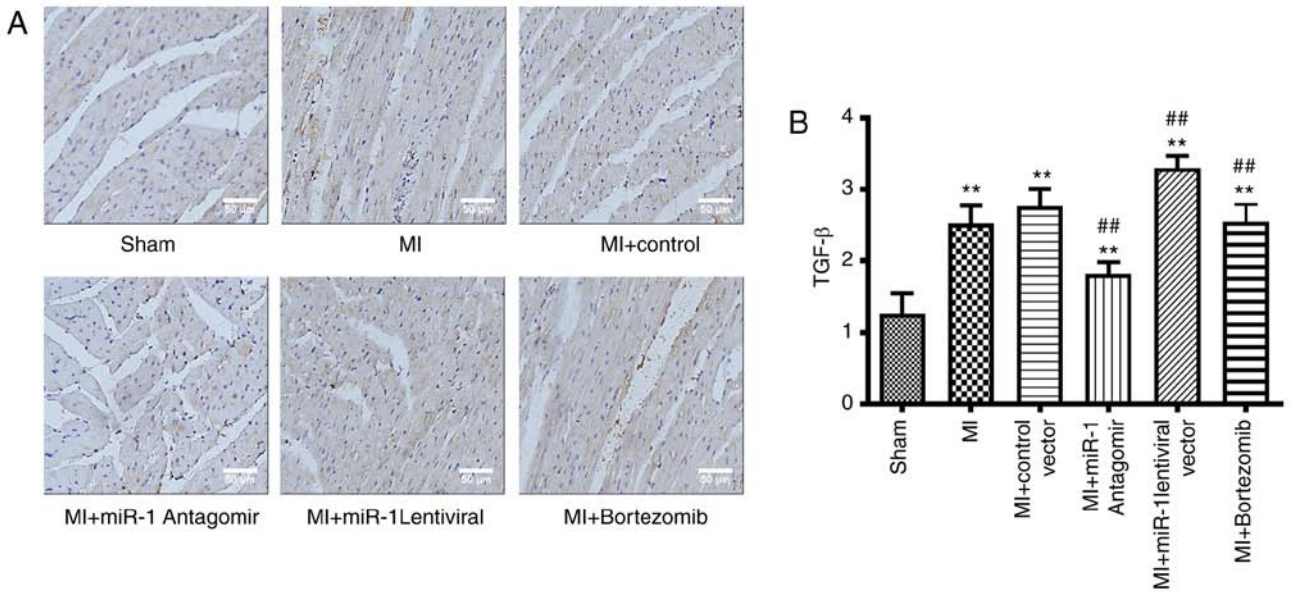


Figure 4. Expression levels of transforming growth factor (TGF)-β in each group. (A) Representative TGF-β expression levels identified via immunohistochemical staining in each group. (B) Quantitative analysis of TGF-β expression in isolated myocardial cardiac tissue in different groups. n=8 mice per group. $^{**}$P<0.01 vs. sham group; $^{\#\#}$P<0.01 vs. MI + control vector group. MI, myocardial infarction.

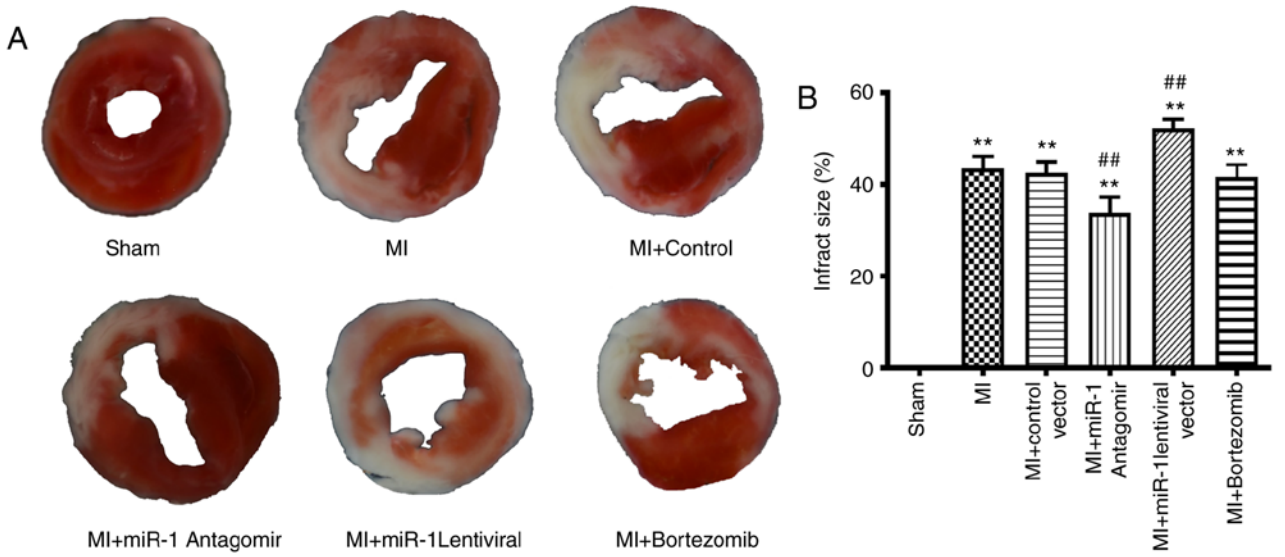


Figure 5. Myocardial infarct size in each group. Representative illustrations of myocardial infarct in different groups. The white area represents myocardial infarct tissue. (A) Myocardial infarct size was calculated and evaluated. (B) The columns and error bars represent mean with standard deviation. n=8 mice per group. $^{**}$P<0.01 vs. sham group; $^{\#\#}$P<0.01 vs. MI + control vector group. MI, myocardial infarction.

significantly improved cardiac function (25). Cheng *et al* (26) revealed that serum miRNA-1 level increased rapidly following acute MI, reaching a peak value at 6 h, indicating a strong positive correlation between serum miRNA-1 levels and myocardial infarct size. Besser *et al* (27) reported that the miR-1/133a clusters were a prerequisite for maintaining specific functions in heart electrophysiology and may affect electrical conduction.

The UPS involves two steps: First, covalent attachment of ubiquitin to a target protein occurs via a cascade of chemical reactions catalyzed by the ubiquitin-activating enzyme (E1), ubiquitin-conjugating enzymes (E2), and ubiquitin ligases (E3). Second, the combination of ubiquitin proteins is recognized and degraded by the 26S proteasomes, and this is a principal pathway for the degradation of certain abnormal intracellular proteins (14,28,29). The 26S proteasome is composed of a 20S core and two 19S regulatory complexes. The UPS plays an important role in the removal of damaged proteins involved in the regulation of inflammation, cell proliferation and differentiation, signal transduction, transcriptional regulation, apoptosis and DNA repair, as well as other biological functions (30,31). Bortezomib is a dipeptide boronate proteasome inhibitor that reversibly binds to and inhibits the 20S proteasome (32,33).

There are a number of observations suggesting that certain E3-ligases play a key role in myocardial ischemia,

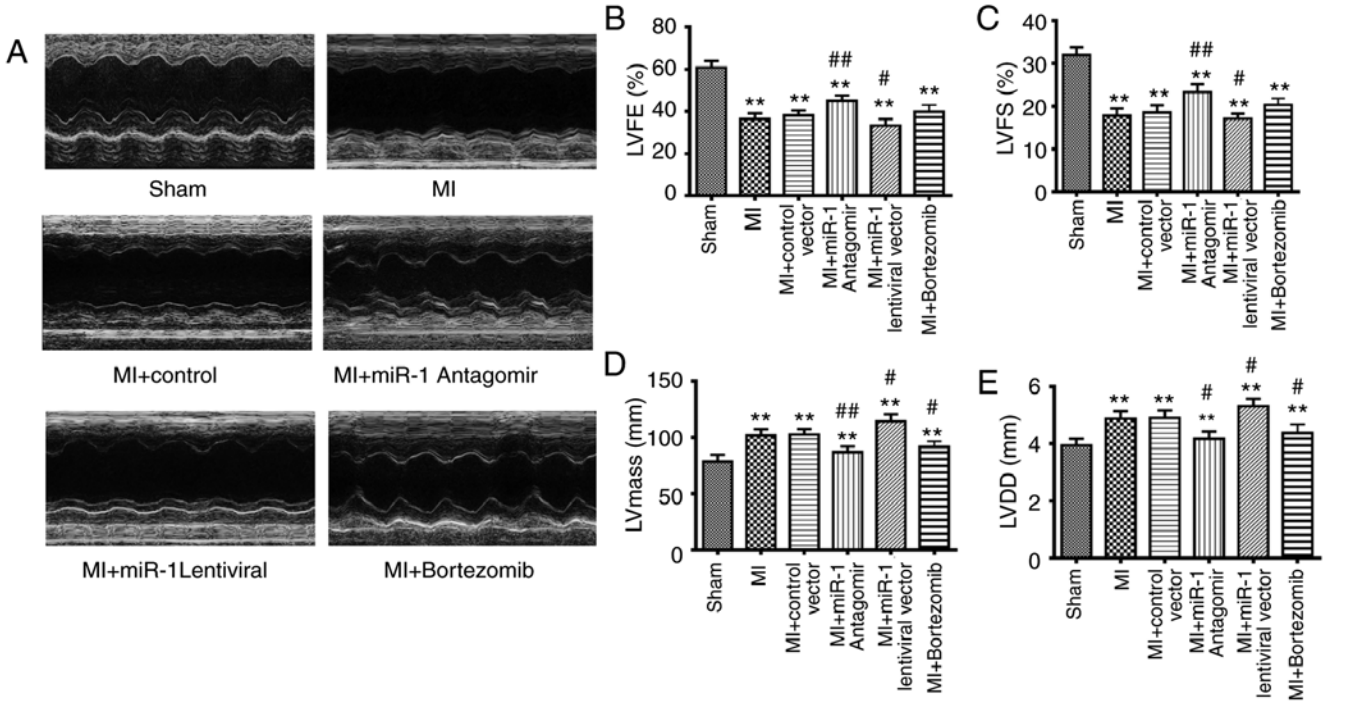


Figure 6. Echocardiographic properties were analyzed. (A) Representative echocardiographic images. (B) LVEF; (C) LVFS; eft ventricular short axis systolic rate; (D) left ventricular weight index (LV mass); (E) LVDD. The columns and error bars represent means and standard deviation. n=8 mice per group. $^{**}$P<0.01 vs. sham group; $^{\#}$P<0.05; $^{\#\#}$P<0.01 vs. MI + control vector group. LVEF, left ventricular ejection fraction; LVFS, left ventricular fractional shortening; LVDD, left ventricular end-diastolic diameter; MI, myocardial infarction.

and that cardiomyocyte apoptosis is closely associated with the abnormal expression of miRNA-1 (6,17). For example, mice that were deficient in a co-chaperone with ubiquitin ligase properties, exhibited an accelerated age-associated pathophysiological phenotype and increased susceptibility to ischemia/reperfusion injury (34,35). miRNA-1 is located within introns 2 and 12 of the E3 ubiquitin-protein ligase. It is possible that the interaction between miRNA and UPS may be involved in the development of cardiovascular disease and myocardial remodeling (36-38); however, this interaction and its possible effects on the cardiovascular system require further investigation. Studies that assess the effect of miRNA-1 on the UPS in the development of heart failure and cardiac remodeling are currently limited.

In the present study, the expression levels of miRNA-1 increased following MI; in addition, miRNA-1 antagomir administration inhibited miRNA-1 expression, and miRNA-1 expression levels increased following injection of the miRNA-1 lentiviral vector, whereas the UPS proteasome blocker bortezomib was unable to modulate miRNA-1 expression. The 19S proteasome, 20S proteasome and ubiquitin ligase E3 in the miRNA-1 antagomir group decreased and then markedly increased following administration of the miRNA-1 lentiviral vector, but only 20S proteasome expression was decreased following delivery of the UPS proteasome blocker. These results demonstrated that miRNA-1 is able to affect all components of the UPS, while the UPS proteasome blocker bortezomib primarily affects the 20S proteasome. The miRNA-1 antagomir and bortezomib both alleviated the ultrastructural impairments, as demonstrated by a decreased LVDD and LV mass, but the effects of the miRNA-1 antagomir were more noticeable and also increased LVEF and LVFS. Furthermore, the opposite effect was observed in the miRNA-1 lentiviral vector group.

Cardiomyocyte apoptosis is one of the major pathological mechanisms underlying MI. Blocking the apoptosis process may prevent the loss of contractile cells and minimize cardiac injury. Thus, a TUNEL staining assay was performed and caspase-3 activity was measured using western blotting to investigate the underlying molecular mechanisms responsible for the improvement in cardiac function induced by administration of the miRNA-1 antagomir. The results indicated that the miRNA-1 antagomir inhibited cardiomyocyte apoptosis, as demonstrated by a decrease in TUNEL-positive cardiomyocytes and decreased caspase-3 expression levels, whereas the UPS proteasome blocker exerted no marked effect. By contrast, miRNA-1 lentiviral vector administration increased cardiomyocyte apoptosis and exacerbated myocardial injury. Masson's trichrome staining and TGF-β expression levels may be used to assess the degree of myocardial fibrosis and myocardial remodeling (39). In the present study, the decreased TGF-β expression levels in the miRNA-1 antagomir group compared with the control group indicate that miRNA-1 antagomir can inhibit fibrosis after myocardial infarction, while bortezomib did not exert noticeable effects. However, the administration of the miRNA-1 lentiviral vector enhanced the fibrotic responses.

A previous study reported that miRNA-1 levels are likely increased in the early stages of heart failure, that overexpression of miRNA-1 aggravates $H_2O_2$-induced cardiomyocyte apoptosis, while inhibition of miRNA-1 using antisense inhibitory oligonucleotides results in marked resistance to $H_2O_2$ (40). It was previously hypothesized that miRNA changes that occur

in the early phase of myocardial ischemia may be associated with cell death and oxidative stress, while those miRNAs altered in the later phase may contribute to post-infarct remodeling or function as compensatory mechanisms (41,42). Naga Prasad *et al* (43) selected a surgical mouse model of transverse aortic constriction to analyze alterations in eight miRNAs upon initiation of cardiac dysfunction, and discovered that the expression of miRNA-1 was decreased in end-stage heart failure. Profiling miRNAs across various tissues revealed that miRNA-1, let-7, miR-26a, miR-30c, miR-126-3p and miR-133 are highly expressed in the murine heart (44). The UPS regulates fundamental cell functions, including mitosis, DNA replication and repair, cell differentiation and transcriptional regulation, as well as receptor internalization, which all play crucial roles in heart biology (29). A previous study (17) demonstrated that the UPS function in patients with heart failure is altered, the protein degradation rate is reduced, and the balance between myocardial protein synthesis and degradation is disrupted, thus leading to an accumulation of modified proteins. UPS proteasome blockers were shown to inhibit nuclear factor-κB and exerted an anti-inflammatory cardioprotective effect. In addition, inadequate coupling between ubiquitination and proteasomal degradation appeared to be a major causative factor behind the UPS functional deficit that contributes to myocardial ischemic injury (45,46).

The present study indicated that the miRNA-1 antagomir exerted a significant protective effect on heart function, decreasing cardiomyocyte apoptosis and alleviating myocardial fibrosis and remodeling. The miRNA-1 antagomir exerted more prominent effects compared with the UPS proteasome blocker bortezomib. Studies on the association between miRNA-1 and UPS are rare. A microRNA/ubiquitin ligase feedback loop was shown to regulate slug-mediated invasion in breast cancer (47). Another previous study identified a novel pathophysiological circuit in the heart, which caused increased miR-199a expression levels and, subsequently, impairment of the UPS that disrupted the miRNAs present in the early phase of myocardial ischemia, which may be associated with cardiomyocyte sarcomere structure and impairment via the release of asymmetric dimethylarginine (36). It was also revealed in the present study that miRNA-1 was able to modulate ubiquitin ligase E3 expression levels. One of the possible underlying molecular mechanisms that has been proposed is that miRNA-1 exerts its effects at the regulated transcriptional and post-transcriptional levels, thus controlling UPS expression and markedly affecting the various components of the UPS. Furthermore, the UPS was markedly involved in alleviating collagen hyperplasia and decreasing apoptosis at the protein level during cardiac remodeling.

In conclusion, the results of the present study suggest that the ubiquitin proteasomes may be the most important mediator of miRNA-1 in the regulation of heart remodeling. miRNA-1 was found to be associated with extensive expression of the UPS components in the myocardium, resulting primarily in changes in ubiquitin ligase E3 expression, leading to the accumulation of proteins, formation of a large number of ubiquitin-positive protein aggregates, increased myocardial cell apoptosis, and myocardial fibrosis or remodeling. Conversely, the miRNA-1 antagomir exerted a significant cardioprotective effect compared with the UPS proteasome blocker bortezomib. Thus, the present study underlines the fact that antisense silencing of miRNA-1 sequences that play a regulatory role in the development of heart failure may be a potential breakthrough in the treatment of heart failure.

**Acknowledgements**

Not applicable.

**Funding**

The present study was supported by the National Natural Science Foundation of China (grant no. 81200158), the Tianjin Health Bureau Key Project Fund (grant no. 16KG155) and the Tianjin Chronic Disease Prevention and Treatment Key Project (grant no. 16ZXMJSY00060).

**Availability of materials and data**

The datasets used or analyzed during the present study are available from the corresponding author on reasonable request.

**Authors' contributions**

LW and XQ designed the experiments. LW and YZ drafted the manuscript. LW performed the experiments and collected the data. XS, YL and YX analyzed the data and generated the figures. All authors have read and approved the final version of the manuscript.

**Ethics approval and consent to participate**

The study protocol was approved by the Animal Ethics Committee of Tianjin Union Medical Center.

**Patient consent for publication**

Not applicable.

**Competing interests**

All the authors confirm that they have no competing interests.

**References**

1. Senni M, Paulus WJ, Gavazzi A, Fraser AG, Díez J, Solomon SD, Smiseth OA, Guazzi M, Lam CS, Maggioni AP, *et al*: New strategies for heart failure with preserved ejection fraction: The importance of targeted therapies for heart failure phenotypes. Eur Heart J 35: 2797-2815, 2014.
2. Majmudar MD, Keliher EJ, Heidt T, Leuschner F, Truelove J, Sena BF, Gorbatov R, Iwamoto Y, Dutta P, Wojtkiewicz G, *et al*: Monocyte-directed RNAi targeting CCR2 improves infarct healing in atherosclerosis-prone mice. Circulation 127: 2038-2046, 2013.
3. Varela A, Mavroidis M, Katsimpoulas M, Sfiroera I, Kappa N, Mesa A, Kostomitsopoulos NG and Cokkinos DV: The neuroprotective agent rasagiline mesylate attenuates cardiac remodeling after experimental myocardial infarction. ESC Heart Fail 4: 331-340, 2017.
4. Sharp TE III, Schena GJ, Hobby AR, Starosta T, Berretta RM, Wallner M, Borghetti G, Gross P, Yu D, Johnson J, *et al*: Cortical bone stem cell therapy preserves cardiac structure and function after myocardial infarction. Circ Res 121: 1263-1278, 2017.

5. Nagpal V, Rai R, Place AT, Murphy SB, Verma SK, Ghosh AK and Vaughan DE: MiR-125b is critical for fibroblast-to-myofibroblast transition and cardiac fibrosis. Circulation 133: 291-301, 2016.
6. Hodgkinson CP, Kang MH, Dal-Pra S, Mirotsou M and Dzau VJ: MicroRNAs and cardiac regeneration. Circ Res 116: 1700-1711, 2015.
7. Zhang J, Lang Y, Guo L, Pei Y, Hao S, Liang Z, Su G, Shu L, Liu H, Huang C and Xu J: MicroRNA-323a-3p promotes pressure overload-induced cardiac fibrosis by targeting TIMP3. Cell Physiol Biochem 50: 2176-2187, 2018.
8. Lee YE, Hong CY, Lin YL and Chen RM: MicroRNA-1 participates in nitric oxide-induced apoptotic insults to MC3T3-E1 cells by targeting heat-shock protein-70. Int J Biol Sci 11: 246-255, 2015.
9. Martinez EC, Lilyanna S, Wang P, Vardy LA, Jiang X, Armugam A, Jeyaseelan K and Richards AM: MicroRNA-31 promotes adverse cardiac remodeling and dysfunction in ischemic heart disease. J Mol Cell Cardiol 112: 27-39, 2017.
10. McIlwain DR, Berger T and Mak TW: Caspase functions in cell death and disease. Cold Spring Harb Perspect Biol 5: a008656, 2013.
11. Communal C, Sumandea M, de Tombe P, Narula J, Solaro RJ and Hajjar RJ: Functional consequences of caspase activation in cardiac myocytes. Proc Natl Acad Sci USA 99: 6252-6256, 2002.
12. Park JK, Doseff AI and Schmittgen TD: MicroRNAs targeting caspase-3 and-7 in PANC-1 cells. Int J Mol Sci 19: E1206, 2018.
13. Bozi LHM and Campos JC: Targeting the ubiquitin proteasome system in diabetic cardiomyopathy. J Mol Cell Cardiol 109: 61-63, 2017.
14. Powell SR, Herrmann J, Lerman A, Patterson C and Wang X: The ubiquitin-proteasome system and cardiovascular disease. Prog Mol Biol Transl Sci 109: 295-346, 2012.
15. Schmidt M and Finley D: Regulation of proteasome activity in health and disease. Biochim Biophys Acta 1843: 13-25, 2014.
16. Gilda JE and Gomes AV: Proteasome dysfunction in cardiomyopathies. J Physiol 595: 4051-4071, 2017.
17. Han QY, Wang HX, Liu XH, Guo CX, Hua Q, Yu XH, Li N, Yang YZ, Du J, Xia YL and Li HH: Circulating E3 ligases are novel and sensitive biomarkers for diagnosis of acute myocardial infarction. Clin Sci (Lond) 128: 751-760, 2015.
18. Zhang M, Sun D, Li S, Pan X, Zhang X, Zhu D, Li C, Zhang R, Gao E and Wang H: Lin28a protects against cardiac ischaemia/reperfusion injury in diabetic mice through the insulin-PI3K-m TOR pathway. J Cell Mol Med 19: 1174-1182, 2015.
19. Wei L, Sun D, Yin Z, Yuan Y, Hwang A, Zhang Y, Si R, Zhang R, Guo W, Cao F and Wang H: A PKC-beta inhibitor protects against cardiac microvascular ischemia reperfusion injury in diabetic rats. Apoptosis 15: 488-498, 2010.
20. Romaine SP, Tomaszewski M, Condorelli G and Samani NJ: MicroRNAs in cardiovascular disease: An introduction for clinicians. Heart 101: 921-928, 2015.
21. Wong LL, Wang J, Liew OW, Richards AM and Chen YT: MicroRNA and heart failure. Int J Mol Sci 17: 502, 2016.
22. Bronze-da-Rocha E: MicroRNAs expression profiles in cardiovascular diseases. Biomed Res Int 2014: 985408, 2014.
23. Li J, Dong X, Wang Z and Wu J: MicroRNA-1 in cardiac diseases and cancers. Korean J Physiol Pharmacol 18: 359-363, 2014.
24. Hao YL, Fang HC, Zhao HL, Li XL, Luo Y, Wu BQ, Fu MJ, Liu W, Liang JJ and Chen XH: The role of microrna-1 targeting of mapk3 in myocardial ischemia-reperfusion injury in rats undergoing sevoflurane preconditioning via the PI3k/Akt pathway. Am J Physiol Cell Physiol 315: C380-C388, 2018.
25. Glass C and Singla DK: MicroRNA-1 transfected embryonic stem cells enhance cardiac myocyte differentiation and inhibit apoptosis by modulating the PTEN/Akt pathway in the infarcted heart. Am J Physiol Heart Circ Physiol 301: H2038-H2049, 2011.
26. Cheng Y, Tan N, Yang J, Liu X, Cao X, He P, Dong X, Qin S and Zhang C: A translational study of circulating cell-free microRNA-1 in acute myocardial infarction. Clin Sci (Lond) 119: 87-95, 2010.
27. Besser J, Malan D, Wystub K, Bachmann A, Wietelmann A, Sasse P, Fleischmann BK, Braun T and Boettger T: MiRNA-1/133a clusters regulate adrenergic control of cardiac repolarization. PLoS One 9: e113449, 2014.
28. Portbury AL, Ronnebaum SM, Zungu M, Patterson C and Willis MS: Back to your heart: Ubiquitin proteasome system-regulated signal transduction. J Mol Cell Cardiol 52: 526-537, 2012.
29. Pagan J, Seto T, Pagano M and Cittadini A: Role of the ubiquitin proteasome system in the heart. Circ Res 112: 1046-1058, 2013.
30. Barac YD, Emrich F, Krutzwakd-Josefson E, Schrepfer S, Sampaio LC, Willerson JT, Robbins RC, Ciechanover A, Mohr FW, Aravot D and Taylor DA: The ubiquitin-proteasome system: A potential therapeutic target for heart failure. J Heart Lung Transplant 36: 708-714, 2017.
31. Divald A, Kivity S, Wang P, Hochhauser E, Roberts B, Teichberg S, Gomes AV and Powell SR: Myocardial ischemic preconditioning preserves postischemic function of the 26S proteasome through diminished oxidative damage to 19S regulatory particle subunits. Circ Res 106: 1829-1838, 2010.
32. Liu N, Liu C, Li X, Liao S, Song W, Yang C, Zhao C, Huang H, Guan L, Zhang P, *et al*: A novel proteasome inhibitor suppresses tumor growth via targeting both 19S proteasome deubiquitinases and 20S proteolytic peptidases. Sci Rep 4: 5240, 2014.
33. Hussain AS, Hari P, Brazauskas R, Arce-Lara C, Pasquini M, Hamadani M and D'Souza A: Changes in cardiac biomarkers with bortezomib treatment in patients with advanced cardiac amyloidosis. Am J Hematol 90: E212, 2015.
34. Calise J and Powell SR: The ubiquitin proteasome system and myocardial ischemia. Am J Physiol Heart Circ Physiol 304: H337-H349, 2013.
35. Day SM: The ubiquitin proteasome system in human cardiomyopathies and heart failure. Am J Physiol Heart Circ Physiol 304: H1283-H1293, 2013.
36. Haghikia A, Missol-Kolka E, Tsikas D, Venturini L, Brundiers S, Castoldi M, Muckenthaler MU, Eder M, Stapel B, Thum T, *et al*: Signal transducer and activator of transcription 3-mediated regulation of miR-199a-5p links cardiomyocyte and endothelial cell function in the heart: A key role for ubiquitin-conjugating enzymes. Eur Heart J 32: 1287-1297, 2011.
37. Wang H, Lai Y, Mathis BJ, Wang W, Li S, Qu C, Li B, Shao L, Song H, Janicki JS, *et al*: Deubiquitinating enzyme CYLD mediates pressure overload-induced cardiac maladaptive remodeling and dysfunction via downregulating Nrf2. J Mol Cell Cardiol 84: 143-153, 2015.
38. Wang F, Lerman A and Herrmann J: Dysfunction of the ubiquitin-proteasome system in atherosclerotic cardiovascular disease. Am J Cardiovasc Dis 5: 83-100, 2015.
39. Yeh YH, Hsu LA, Chen YH, Kuo CT, Chang GJ and Chen WJ: Protective role of heme oxygenase-1 in atrial remodeling. Basic Res Cardiol 111: 58, 2016.
40. Tang Y, Zheng J, Sun Y, Wu Z, Liu Z and Huang G: MicroRNA-1 regulates cardiomyocyte apoptosis by targeting Bcl-2. Int Heart J 50: 377-387, 2009.
41. Dong S, Cheng Y, Yang J, Li J, Liu X, Wang X, Wang D, Krall TJ, Delphin ES and Zhang C: MicroRNA expression signature and the role of microRNA-21 in the early phase of acute myocardial infarction. J Biol Chem 284: 29514-29525, 2009.
42. Yin C, Salloum FN and Kukreja RC: A novel role of microRNA in late preconditioning: Upregulation of endothelial nitric oxide synthase and heat shock protein 70. Circ Res 104: 572-575, 2009.
43. Naga Prasad SV, Duan ZH, Gupta MK, Surampudi VS, Volinia S, Calin GA, Liu CG, Kotwal A, Moravec CS, Starling RC, *et al*: Unique microRNA profile in end-stage heart failure indicates alterations in specific cardiovascular signaling networks. J Biol Chem 284: 27487-27499, 2009.
44. Lagos-Quintana M, Rauhut R, Yalcin A, Meyer J, Lendeckel W and Tuschl T: Identification of tissue-specific microRNAs from mouse. Curr Biol 12: 735-739, 2002.
45. Hu C, Tian Y, Xu H, Pan B, Terpstra EM, Wu P, Wang H, Li F, Liu J and Wang X: Inadequate ubiquitination-proteasome coupling contributes to myocardial ischemia-reperfusion injury. J Clin Invest 128: 5294-5306, 2018.
46. Adams B, Mapanga RF and Essop MF: Partial inhibition of the ubiquitin-proteasome system ameliorates cardiac dysfunction following ischemia-reperfusion in the presence of high glucose. Cardiovasc Diabetol 14: 94, 2015.
47. Manne RK, Agrawal Y, Bargale A, Patel A, Paul D, Gupta NA, Rapole S, Seshadri V, Subramanyam D, Shetty P and Santra MK: A microRNA/Ubiquitin ligase feedback loop regulates slug-mediated invasion in breast cancer. Neoplasia 19: 483-495, 2017.